THE ANNALS OF "DUNAREA DE JOS" UNIVERSITY OF GALATI.
FASCICLE IX. METALLURGY AND MATERIALS SCIENCE
N^0. 1 – 2011, ISSN 1453 – 083X

CONTINUOUS FLUX THERMAL TREATMENTS FOR IMPROVING THE RESISTANCE AT ALTERNATE BENDING OF MEDIUM TO HIGH STRENGTH STEEL STRIPS

Tiberiu Florian POTECAŞU[1], Octavian POTECAŞU[1], Petrică ALEXANDRU[1], Francisco Manuel BRAZ FERNANDES[2], Rui Jorge CORDEIRO SILVA[2]

[1]Center of Nanostructures and Functional Materials, "Dunărea de Jos" University of Galaţi
[2]CENIMAT/Materials Science Department, Nova University of Lisbon, Caparica, Portugal
email: tpotecasu@gmail.com, opotec@ugal.ro

ABSTRACT

The research was focused on obtaining medium to high strength steel strips for strapping heavy products by applying continuous flux thermal treatments on common grades, cheap carbon steels. For steel strapping the behavior at alternate bending is an important issue, thus an objective of the research was to make sure that the treated products withstand a critical number of alternate bending cycles and further more an improvement of the resistance at alternate bending by applying thermal treatments in continuous flux was pursued.

The paper presents the results of the alternate bending test, SEM fractographs, optical analysis of the fracture surface and surface of the strip in the vicinity of the fracture surface after breaking by alternate bending using a stereo-microscope and optical analysis on etched and un-etched samples in transversal section along the rolling direction in the vicinity of the fracture surface using a metallographic optical microscope; for the following samples: the raw material in strain-hardened state, samples subjected to continuous flux quenching from 900°C and tempering by passing through the furnace maintained at 600°C, and samples subjected to quenching from 900°C and tempering by passing through the furnace maintained at 700°C.

KEYWORDS: carbon steel strips, continuous flux thermal treatments, resistance at alternate bending

1. Introduction

The research was focused on producing steel strips for strapping made from common carbon steels with improved mechanical characteristics by means of thermal treatments.

A good resistance at alternate bending is very important for steel strapping because in practice there are cases where, during transportation of the strapped cargo, as a consequence of stacking and poor road conditions, the strip can have a sliding motion around corners subjecting the material to alternate bending.

In this respect in this paper there are presented the effects on the resistance at alternate bending of the continuous flux thermal treatment of quenching from 900°C and tempering at 600°C for one minute and also of the continuous flux thermal treatment of quenching from 900°C and tempering at 700°C for one minute.

2. The raw material

The chemical composition of the steel used as raw material in the experiments is presented in Table 1.

Table 1. *Chemical composition of the steel used as raw material, [wt%]*

C	Si	**Mn**	P	S	Al	As	Ti
0.185	0.063	**1.350**	0.023	0.008	0.050	0.043	0.005
V	Cu	Ni	Cr	Mo	Nb	B	
0.001	0.012	0.027	0.031	0.002	0.001	0.0001	

The steel is cold-rolled with a thickness of 0.8 mm and cut in strips of 19 mm in width. The results of the tensile strength test done on raw material samples labeled B.0 are presented in Table 2. The samples were not machined for the tensile strength test because of their intended use as steel strapping; the values represent the average of three valid tests (broken in the mid-range of the sample between the grips).

Table 2. *Tensile strength test results for the raw material*

Sample	**Section** [mm x mm]	**Rm** [MPa]	**A_{prop}** [%]	**A_{80mm}** [%]
B.0	0.8 x 19	820	12	8

The Vickers micro-hardness, determined using the 500g weight, of the B.0 raw material samples is 275 HV – the value represents the average value resulting from 8 valid imprints.

At alternate bending at 90° in both directions over a 3 mm radius, the first visible cracks are observed after bending for 6 times and failure takes place after bending for 7 times. The images done with a stereomicroscope on B.0 raw material samples after breaking by alternate bending are presented in Figure 1 and Figure 2. In Figure 1, from the analysis of the aspect of the fracture surface it can be seen that cracks parallel to the surface of the strip with length in the fracture surface of 1 to 2 mm were formed, these are deep and wide, and are present along the whole width of the strip. These cracks do not necessary form a continuous network, but are present especially in the central area (thickness wise). The probable cause that leads to their formation is the strain hardened state of the material, and the presence of non-metallic inclusions flattened during the rolling process; the intergranular interfaces from the plastically deformed metallic mass, or the interfaces between metallic matrix and inclusions present a low degree of coherence and thus shear stress concentrators form with catastrophic effects. Regarding the aspect of the fracture surface towards the surface of the strip there can be seen areas with crystalline-shine aspect that suggest fragile breaking and also round-shape specific reflections that suggest ductile breaking.

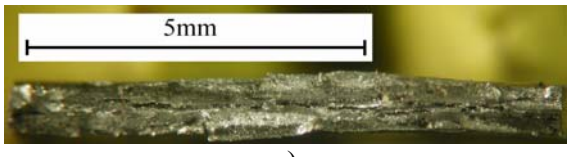

a)

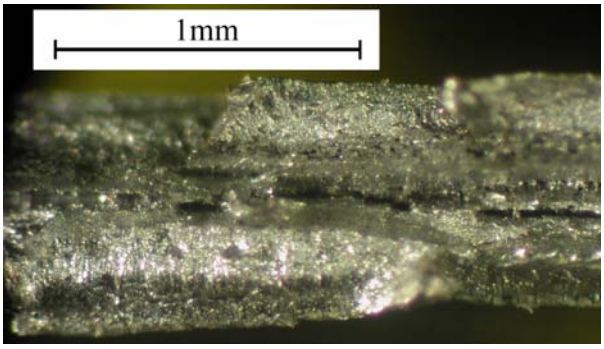

b)

Fig. 1. *The aspect of the fracture surface after breaking by alternate bending specific for type B.0 raw material samples. The images have been taken with a stereomicroscope; b) represents a detail from a).*

From Figure 2, it can be seen that the surface of the strip shows that important deformations took place at a microscopic level in all the bending affected region, not only in the immediate vicinity of the fracture surface.

Thus it is put into evidence the appearance of some oblique upsetting lines at an angle of approximately 7.5° from the normal to the edge of the strip. These lines have formed as a result of the stretching-compression cycles of the material from the surface of the strip.

The upsetting lines have lengths between 2 and 4.5 mm and are more clearly seen in areas with the shape of bands perpendicular to the edge of the strip; observations that suggest the concentration of the deformation forces in these areas. Even more, in the case of some of these horizontal bands cracks can be seen between adjacent upsetting lines. At a distance of approximately 5mm from the fracture surface another area can be observed where a partial fracture took place. Both of these fracture lines (the catastrophic fracture and the partial fracture) were formed by the coalescence of adjacent cracks developed between the upsetting lines.

The fracture line is irregular showing areas where the material detached between two oblique upsetting lines and got curved from the action of the stretching forces from the surface of the material prior to the catastrophic fracture, suggesting that, during the fracture process, important plastic deformations took place simultaneously with the formation of a great number of independent cracks. In this way, critical sections were created with a role of tension concentrators that ultimately lead to catastrophic failure.

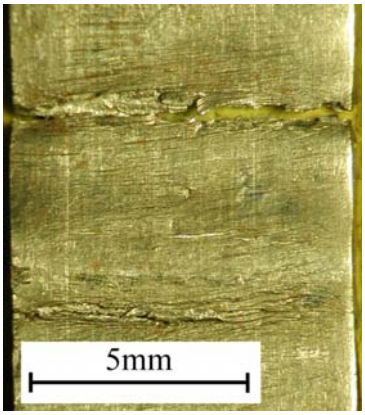

a)

b)

Fig. 2. *The aspect of the surface of the strips after breaking by alternate bending, specific for type B.0 raw material samples. The images have been taken with a stereomicroscope; b) represents a detail from a).*

In Figure 3, SEM details of the fracture surface are presented taken from an area close to the right edge of the fracture surface. The detail taken at x100 magnification covers the whole thickness of the steel strip.

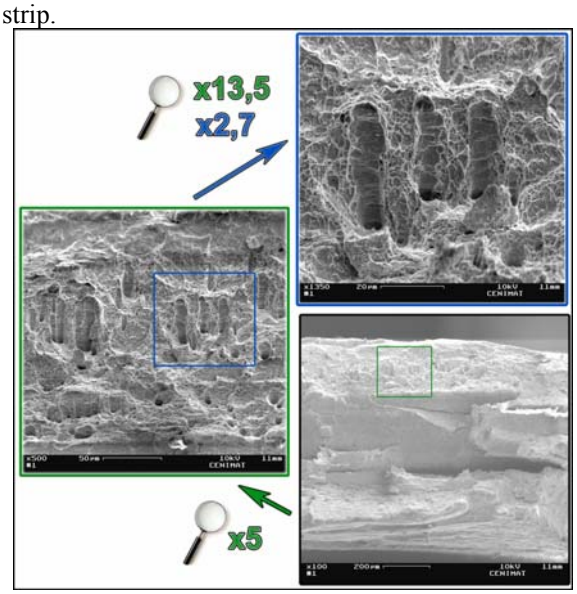

Fig. 3. *The specific aspect of some details of the breaking surface after breaking by alternate bending for type B.0 raw material samples. Images taken with SEM.*

As it was put into evidence in the pictures taken with the stereo-microscope, it can be seen that the fracture presents different aspects along the thickness of the strip. Thus, as also seen in the details taken at higher magnifications, in the upper part, the fracture surface presents characteristics specific for dimple rupture – these dimples are very shallow towards the surface of the strip indicating a mostly fragile rupture, towards the center, the dimples get more pronounced and are circular in shape indicating a mostly ductile rupture. On the surface of the strip areas indicating decohesive rupture at the interface between inclusions and the metallic matrix are also present – these are shaped as channels longitudinally oriented.

In Figure 4, a microstructure is presented realized on longitudinal section in the vicinity of the fracture section; the sample was not etched and the optical magnification was x200.

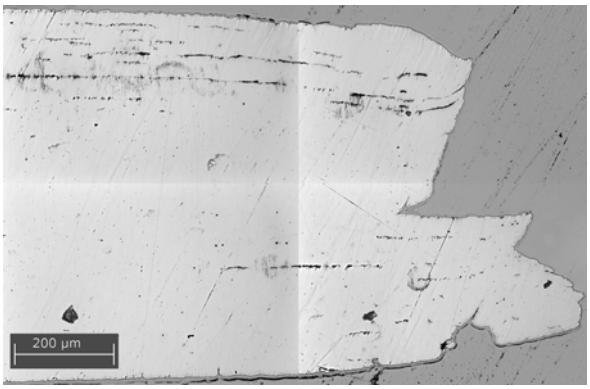

Fig. 4. *Microstructure done in longitudinal section on the lamination direction, from the area adjacent to the fracture surface after breaking by alternate bending; microstructure characteristic for type B.0 raw material samples. The image was done on unattached sample by digital composition of 4 adjacent photos taken at x200 optical magnification.*

Two interesting aspects can be observed in the image. Firstly, the presence of dark lines with a thickness of approximately 7-8 µm, parallel to the surface of the strip is observed. The study of the inclusions arranged in lines on samples not subjected to alternate bending showed that they have a thickness between 0.5 to 2 µm, exceptionally isolated polygonal formations can be observed that can go up to 4-5 µm. Thus it can be concluded that as a result of the alternate bending these lines are "thickened". In fact this "thickening" is the effect of the decohesive rupture that takes place at the interface between the inclusion lines and the metallic matrix. Secondly, the role of these longitudinal cracks in joining transversal cracks with catastrophic consequences is observed

from the contour of the fracture surface in this section.

3. The continuous flux thermal treatment installation

For the experiments, a laboratory installation was designed and built in order to apply continuous flux thermal treatments on the steel strips. The installation is presented in Figure 5 in a schematic representation showing its functional blocks, their placement and inter-relations.

The laboratory installation was connected to a computerized control and measurement system. The parameters that were subjected to computerized control were:

- temperature of the austenitizing furnace;
- the speed of the steel strip through the system;
- the temperature and pressure of the cooling water;

Also a device was used to set and maintain at a constant value the flow of the protection gas fed into the muffle of the austenitizing furnace.

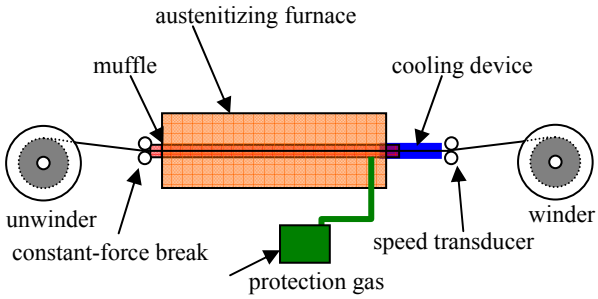

Fig. 5. *Schematic representation of the laboratory installation used for experimental research of continuous flux thermal treatments of steel strips.*

4. Experimental results

4.1.Continuous flux quenching from 900°C and tempering for one minute at 600°C

4.1.1. Presentation of the thermal treatment

The type B.1 samples were subjected to continuous flux quenching thermal treatment by heating for complete austenitization in the furnace maintained at 900°C. The steel strips' speed was maintained at 2 m/min which means that a finite section of steel strip passing through the furnace will be kept at the furnace's temperature for one minute.

The cooling for quenching was done by water jets at room temperature (20°C) and constant pressure.

After quenching, also in continuous flux the steel strip was subjected to the tempering thermal treatment by passing through the furnace maintained at 600°C. The steel strips' speed, as the treatment was applied in continuous flux, was also of 2 m/min, thus the duration that a finite section of steel strip is maintained at the furnace's temperature is also of one minute. After the exit from the tempering furnace the steel strip was cooled with water showers.

In Figure 6 it is presented the result of the simulation which shows the variation of the temperature for a finite section of steel strip with the section of 0.8x19 mm while passing through the tempering furnace maintained at 600°C. In the figure, markers were introduced at 33 seconds when the temperature of the steel strip is estimated at 402°C and at the exit from the tempering furnace, at 60 seconds when the steel strip's temperature is estimated at 563°C.

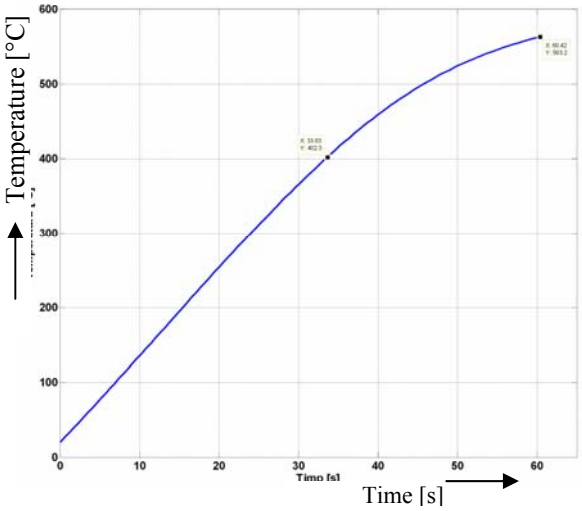

Fig. 6. *Simulation that shows the evolution of the temperature inside the steel strip as a function of time during the tempering of 0.8x19mm steel strip inside the furnace maintained at 600°C for one minute – type B.1 samples. Markers at: 33s-402°C and 60s-563°C.*

4.1.2. Mechanical properties

The results of the tensile strength test are presented in Table 3.

Table 3. *The tensile strength results for the samples treated by continuous flux quenching from 900°C and tempering at 600°C*

Sample type	**Section** [mm x mm]	**Rm** [MPa]	**A_{prop}** [%]	**A_{80mm}** [%]
B.1	0.8 x 19	814	16.4	10.6

It can be seen that the tensile strength is comparable to that of the raw material, but the breaking elongation is improved by 32.5%.

The Vickers micro-hardness, determined using the 500g weight, of the B.1 samples is 293 HV – the value represents the average result from 8 valid imprints.

4.1.3. Resistance at alternate bending

At alternate bending, the first cracks are observed after bending for 6 times and failure takes place after bending for 7 times. The results are the same with the ones obtained for the type B.0 raw material samples, even though the breaking elongation is significantly improved.

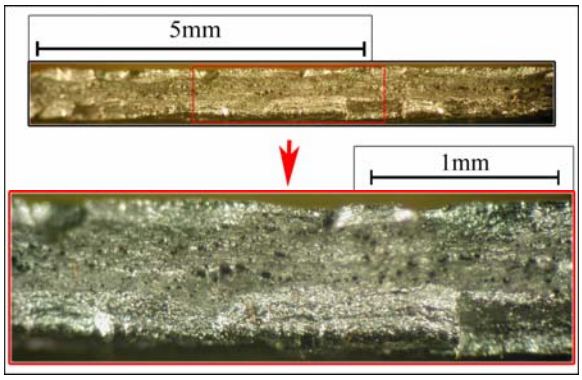

Fig. 7. *The aspect of the breaking surface after breaking by alternate bending specific for type B.1 samples subjected to quenching from 900°C and tempered for one minute in the furnace maintained at 600°C. The images have been taken with a stereomicroscope.*

The aspect of the fracture surface after breaking by alternate bending is presented in Figure 7. From the images it can be seen that the relief of the fracture surface has a preferential orientation parallel to the surface of the strip.

The way the light is reflected from the fracture surface is specific for light reflection from curved surfaces indicating a ductile fracture. Also some small conical craters are observed that indicate a local ductile rupture of cone-cup type.

Having dimensions larger than these craters, on the median area on the whole width of the strip, dark areas with a slightly rectangular shape can be noticed; these are arranged in rows, sometimes linked together by finer cracks reaching lengths of approximately 0.2 mm.

By their shape and distribution, these cracks indicate that they formed at the interface between inclusions and the metallic matrix during the alternate bending cycles, possibly contributing to the ultimate failure.

The relief on an overall view is irregular and presents shapes that indicate a flow of material, the rupture was mainly ductile.

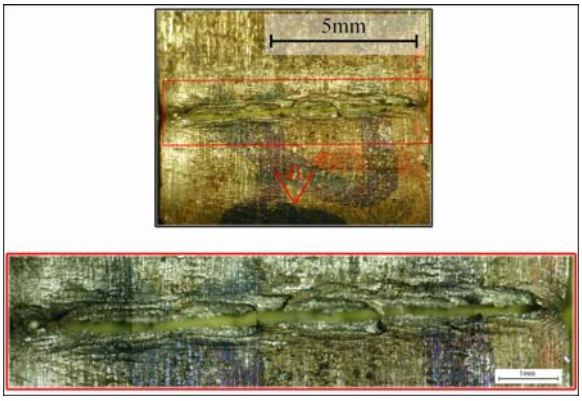

Fig. 8. *The aspect of the surface of the strips after breaking by alternate bending, specific for type B.1 samples subjected to quenching from 900°C and tempered for one minute in the furnace maintained at 600°C. The images have been taken with a stereomicroscope.*

In Figure 8 the aspect of the surface of the steel strip in the vicinity of the fracture line after breaking by alternate bending is presented. In the images, it can be noticed that on the surface of the strip upsetting lines have formed as a result of the stretching-compression cycles of the material from the surface during the alternate bending. These upsetting lines are parallel to the fracture line. Also some finer upsetting lines can be observed; these later lines are inclined at approximately 14° from the normal to the edge of the strip. In the immediate vicinity of the fracture line cracks can be noticed between adjacent upsetting lines. Also, this kind of cracks formed between upsetting lines parallel to the fracture line, but much finer, can also be noticed in another area at approximately 4 mm in the rolling direction, relatively centered to the width of the strip. In the image showing the detail of the fracture surface it can be noticed how the material from the surface of the strip has some twisted and stretched prominences on both sides of the fracture line that indicate that the rupture has taken place by the propagation in profundity of some individual cracks, relatively aligned, starting from the surface of the strip, propagation that had the effect of concentrating the deformation tensions in the sections of material between these cracks, leading implicitly to the catastrophic failure, ductile by overload.

4.2. Continuous flux quenching from 900°C and tempering for one minute at 700°C

4.2.1. Presentation of the thermal treatment

The type B.2 samples were subjected to continuous flux quenching thermal treatment by

heating for complete austenitization in the furnace maintained at 900°C. The steel strips' speed was maintained at 2 m/min which means that a finite section of steel strip passing through the furnace is kept at the furnace's temperature for one minute.

The cooling for quenching was done by water jets at room temperature (20°C) and constant pressure.

After quenching, also in continuous flux the steel strip was subjected to the tempering thermal treatment by passing through the furnace maintained at 700°C. The steel strips' speed, as the treatment was applied in continuous flux, was also 2 m/min, thus the duration that a finite section of steel strip is maintained at the furnace's temperature is also one minute. After the exit from the tempering furnace the steel strip was cooled with water showers. In Figure 9 it is presented the result of the simulation which shows the variation of the temperature for a finite section of steel strip with the section of 0.8x19 mm while passing through the tempering furnace maintained at 700°C. In the figure, markers were introduced at 22s-404°C, 36s-602°C and at the exit from the tempering furnace: 60s-690°C. It can be seen that the radiative heat transfer gets more intense as the temperature of the steel strip at the exit is getting closer to the temperature of the furnace.

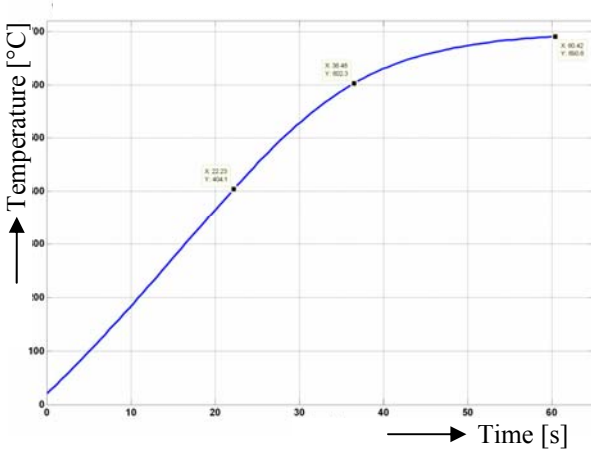

Fig. 9. *Simulation that shows the evolution of the temperature inside the steel strip as a function of time during the tempering of the 0.8x19mm steel strip inside the furnace maintained at 700°C for one minute – type B.2 samples. Markers at: 22s-404°C, 36s-602°C, 60s-690°C.*

4.2.2. Mechanical properties

The results of the tensile strength test are presented in Table 4.

Table 4: The tensile strength results for the samples treated by continuous flux quenching from 900°C and tempering at 700°C

Sample type	**Section** [mm x mm]	**Rm** [MPa]	**A_{prop}** [%]	**A_{80mm}** [%]
B.1.5	0.8 x 19	700	21.5	14.3

It can be seen that the tensile strength is reduced by 14% compared to that of the raw material, but the breaking elongation is improved by 78.8%.

The Vickers micro-hardness, determined using the 500g weight, of the B.2 samples is 235 HV – the value represents the average result from 8 valid imprints.

4.2.3. Resistance at alternate bending

At alternate bending, the first cracks are observed after bending for 8 times, and failure takes place after 11 alternate bending cycles.

In Figure 10 there are presented images taken with a stereomicroscope from the fracture surface after breaking by alternate bending. From the images it can be seen that the relief of the fracture surface is irregular, the height variations of the topographical formations are generally smooth and small. The way the light is reflected from the fracture surface indicates that the fracture surface is made out of small rounded surfaces which indicates that a flow of material took place, thus the rupture was mostly ductile. On the surface black dots are observed, especially in the median area from the thickness of the strip; these are of two different types. There are some small craters with circular shape suggesting a cone-cup ductile rupture and some dark areas with a slightly rectangular contour that suggests the presence of a crack parallel with the surface of the strip – these latter ones are sometimes grouped, forming cracks with lengths of 0.1 mm to 0.2 mm.

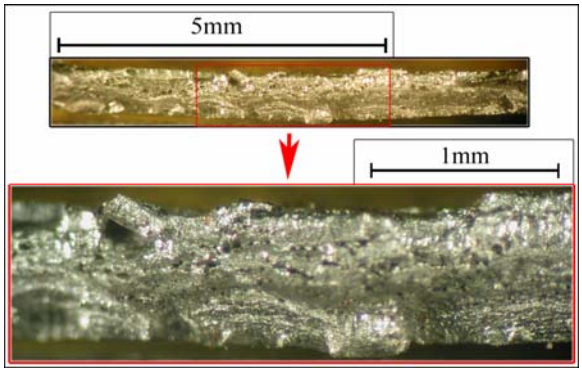

Fig. 10. *The aspect of the breaking surface after breaking by alternate bending specific for type B.2 samples subjected to quenching from 900°C and tempered for one minute in the furnace maintained at 700°C. The images have been taken with a stereomicroscope.*

In Figure 11 it is presented the surface of the steel strip in the vicinity of the fracture line after breaking by alternate bending; the images are taken with a stereo-microscope. It can be seen that on the surface of the strip cracks have been formed perpendicular to the edge of the strip in the whole area affected by alternate bending; generally the cracks are fine, but they get more pronounced in the immediate vicinity of the fracture line and in another area some 4 mm away from the fracture line in the rolling direction. The fracture line describes a straight line. In the immediate vicinity of the fracture line, deep cracks parallel with the fracture line can be observed. Also signs of material being pulled off between the opposite sides of the fracture line can be noticed; this suggests that, at the moment of the ultimate failure, some bridges still existed that maintained the continuity of the material. From all these observations it can be concluded that the rupture was caused by the development of cracks from the surface of the strip, perpendicular to the edge, cracks that had a role of stress concentrators on some critical sections, sections where the rupture was ductile by overloading.

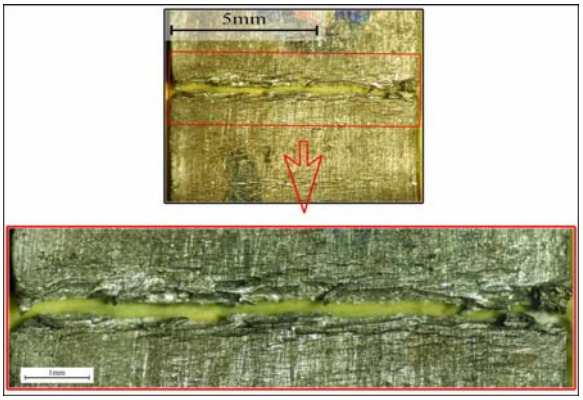

Fig. 11. *The aspect of the surface of the strips after breaking by alternate bending, specific for type B.2 samples subjected to quenching from 900°C and tempered for one minute in the furnace maintained at 700°C. The images have been taken with a stereomicroscope.*

The SEM details presented in Figure 12 explain very well the rupture mechanism involving the development of cracks from the surface of the strip followed by ductile rupture by overload. The main image taken at x120 magnification contains the whole thickness of the strip and is taken from a region close to the left edge of the fracture surface. In the image, it can be noticed that the fracture surface presents relatively large regions where the rupture took place by different mechanisms. There is one region which starts from the surface of the strip going towards the middle with a shape that can be approximated with a triangle; this region has a uniform nuance and presents a generally featureless topography. The image from top-right shows a detail from this region taken at x1000 magnification. In this detail it can be noticed that the surface has a series of lines that ramify like rivers, lines characteristic to cleavage rupture – fragile rupture. Thus it can be said that this region represents a crack that formed in the material after strain hardening as a result of the alternate bending cycles. On the other hand, the detail taken at x500 magnification presented in the bottom-right image from Figure 12 is taken from the top-left region of the main image (taken at x120 magnification). In this second detail, the fracture surface has conical craters with different sizes and different depths, specific for ductile dimple rupture by overload. In some of these craters, at their bottom, a spherical carbide particle can be noticed – where the micro-void nucleated.

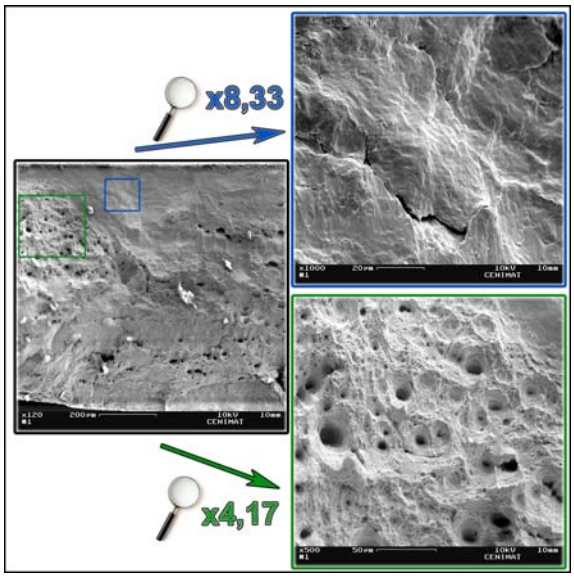

Fig. 12. *SEM details of the breaking surface after breaking by alternate bending characteristic for type B.2 samples subjected to quenching from 900°C and tempered for one minute in the furnace maintained at 700°C.*

In Figure 13 there are presented a microstructure taken at x100 magnification and details from that main microstructure taken at x1000 optical magnification; the images are taken in the vicinity of the fracture surface in longitudinal section in the rolling direction, after breaking by alternate bending. Besides the fracture line, 3 cracks can be noticed that start from the surface of the strip towards the center, cracks that are presented in detail at x1000 optical magnification. One crack of this type is observed in the bottom-right region of the main image. It has a

depth of approximately 18 µm, it has a rectangular profile with a width of approximately 2 µm. It can be noticed that the crack stopped on a formation of free ferrite. Also in the bottom region, to the left, there is another crack starting from the surface of the strip towards to center. This crack has a depth of approximately 91 µm and has an irregular shape, with an opening at the surface of the strip of approximately 30 µm. Between this crack and the fracture surface there is a distance of approximately 74 µm, and the shape of the structural constituents in-between shows that the material was compressed. A third crack is located in the top side of the main image. It has a depth of approximately 37 µm and a width at the surface of the strip of approximately 24 µm.

The structural constituents located in the immediate vicinity of the vertical walls of the crack indicate that they suffered a deformation caused by the compression forces during the alternate bending cycles. The relatively large width of this crack and its shape – approximately rectangular – indicates that it formed during early stages of the alternate bending cycles, thus it had time to get wider by compressing the adjacent material. Also it can be noticed that the crack does not have a typical "V" shape profile, it is close to a "U" profile. This thing can be explained by the fact that the stretching forces caused by the bending cycles following the formation of the crack have stretched the material from the whole transversal section containing the crack.

The conclusion that rises from this observation is the fact that, as a consequence of the chemical inhomogeneity of the material, the propagation of the cracks started from the surface of the strip is stopped very efficiently by the islands of free ferrite, and even more they are not re-activated by the continuation of the destructive forces.

Regarding the profile of the fracture surface, from the images presented in Figure 13 it can be seen that the cracks that form at the interface between inclusions and the metallic matrix have an important role in the ultimate failure. These cracks lead to a step-like fracture surface profile, by linking cracks developed in transversal direction developed in different sections.

Depending on their depth and opening, it can be noticed that some of these cracks have formed during the early stages of the alternate bending cycles, some others have formed during the late stages of the alternate bending cycles and some have formed when the ultimate failure took place.

One of the cracks formed during the early stages of the alternate bending cycles is presented in detail in the image from top-left. The crack has a depth of approximately 114 µm and an opening at the fracture surface of approximately 23 µm. It can be noticed that the line of the upper wall of the crack describes a sinuous profile in comparison to the profile of the lower wall of the crack which describes an arc with large radius.

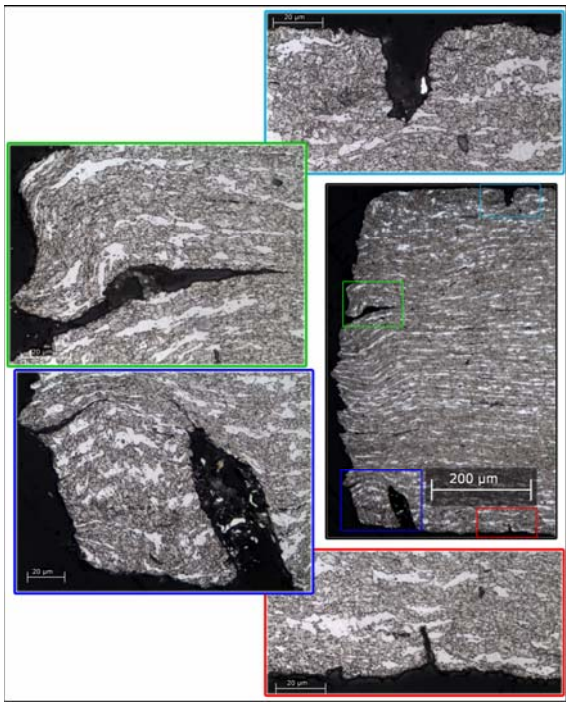

Fig. 13. *Microstructures done in longitudinal section on the lamination direction, from the area adjacent to the breaking surface after breaking by alternate bending; microstructures characteristic for type B.2 samples subjected to quenching from 900°C and tempered for one minute in the furnace maintained at 700°C. Images done on etched sample with nital 5%, the main image was taken at x100 optical magnification and the details were taken at x1000 optical magnification.*

This difference is also observed in the texture of the microstructural constituents from the material in the upper side of the crack and respectively the lower side. Thus it can be concluded that the rupture in transversal plane took place in successive sequential steps delimited by the location of cracks parallel to the surface of the strip developed at the interface between inclusions and metallic matrix.

All of the above observations show the fact that the cracks parallel to the surface of the strip developed at the interface between inclusions and the metallic matrix and the cracks caused by strain-hardening due to the stretching-compression cycles, they both concur and have an important role in the rupture mechanism of the samples subjected to continuous flux quenching from 900°C and tempering for one minute at 700°C.

5. Conclusions

The steel strips that were in strain-hardened state, also used as raw material for the continuous flux thermally treated samples, showed an unfavorable behavior at alternate bending. Mainly because most of the destructive effects of alternate bending are located inside the material in the entire region affected by alternate bending, and only later, signs of destruction appear on the surface of the strip. The reason for that is the fact that the residual stress from the plastic deformation increases the risk of decohesive rupture at the interface between inclusions and the metallic matrix.

After applying the continuous flux thermal treatment of quenching from 900°C and tempering for one minute by passing through the furnace maintained at 600°C the tensile strength is similar to that of the raw material and the resistance at alternate bending also appears to be similar to that of the raw material in strain-hardened state. But there are considerably less cracks developed at the interface between inclusions and the metallic matrix; thus the damage inside the material with consequences on the tensile strength and elongation are reduced. Also signs of destruction due to alternate bending are more easily observed as the cracks started from the surface of the strip play a more important role in the fracture mechanism.

The resistance at alternate bending is significantly increased after applying the continuous flux thermal treatment of quenching from 900°C and tempering for one minute by passing through the furnace maintained at 700°C. The first cracks are observed after bending for 8 times compared to 6 times for the raw material and failure takes place after bending for 11 times compared to 7 times. Also the tensile strength is reduced down to 700 MPa and the A_{80mm} breaking elongation is increased up to 14.3%. The cracks started from the surface of the strip after strain hardening as a direct consequence of stretching-compression cycles during the alternate bending play an important role in the ultimate failure. The increase in resistance at alternate bending is explained by the fact that these cracks which started from the surface of the strips are stopped by the free ferrite formations occurred during the thermal treatment because of the chemical inhomogeneity within the material caused by the manganese content.

References

[1]. Tiberiu Potecaşu, Octavian Potecaşu, Rui Jorge Cordeiro Silva, *Straps of high resistance processed of steel with low carbon*, Metalurgia Internaţional, Vol XV, No. 4, 2010, pg. 50-53, ISSN 1582-2214;

[2]. ASM Handbook, Volume 12, *Fractography*, published in 1987 as Volume 12 of the 9th Edition *Metals Handbook (second printing 1992)*.

[3]. Madeleine Durand-Charre, *Microstructure of Steels and Cast Irons*, Springer-Verlag Berlin Hidelberg New York, ISBN 3-540-20963-8, Germany, 2004.

[4]. H.K.D.H Bhadeshia, *Bainite in Steels Transformations, Microstructure and Properties 2nd editon*, Cambridge University Press, ISBN 1-86125-112-2, UK, 2001.

[5]. H. K. D. H. Bhadeshia, *Interpretation of the Microstructure of Steels*, http://www.msm.cam.ac.uk/phase-trans/2008/Steel_Microstructure/SM.html